

## Protective Performance and Microstructural Behavior of Asphalt and Tar Coatings on Steel under Varying Chloride Concentrations

Saraa .M. Mohameed<sup>1</sup><sup>1</sup>Project and construction Division, Mustansiriyah University, Baghdad, Iraq.[saraamajeed96@uomustansiriyah.edu.iq](mailto:saraamajeed96@uomustansiriyah.edu.iq)

Received:	7/5/2026	Accepted:	23/6/2026	Published:	28/6/2026
-----------	----------	-----------	-----------	------------	-----------

**Abstract**

The present paper aims to undertake a comparison between the corrosion inhibition effects of asphalt and tar paints used on the surface of steel samples subjected to sodium chloride environments of different concentrations (0.5 M and 1.0 M). This was done by first coating the steel samples before subjecting them to sodium chloride environments for a period of 17 days. Measurements of the weight loss of samples after every 72 hours were made in order to estimate the corrosion rates. The gravimetric technique was employed in determining the corrosion rate in accordance with ASTM G31-21 standards. Other tests such as TDS and SEM were done to study salt concentration levels and microstructure alterations of surfaces. It is noted that there was a steady reduction in both salt concentration and corrosion rates as a result of iron oxide and hydroxides coating on the surface. Asphalt coatings showed a better level of protection against corrosion than tar coatings and untreated samples. The values of the corrosion rates were equal to 0.19 mm/year in 0.5 M NaCl solution and 0.36 mm/year in 1.0 M NaCl solution, while in the case of tar coatings they were equal to 0.28 and 0.52 mm/year correspondingly. SEM micrographs revealed that asphalt coating was dense, homogeneous, and tightly adhering to the surface with few defects, while tar coating was characterized by microcracks and porosities.

**Keywords** :-Corrosion; Asphalt coating; Tar coating; Steel protection; NaCl solution; Corrosion rate; Bituminous materials.

**1. Introduction**

Corrosion, which can be described as either a chemical or an electrochemical reaction between materials and their surroundings, is responsible for the degradation of metals and alloys. In steel constructions, corrosion is costly and presents potential hazards. Studies have estimated that global corrosion-related losses exceed 3% of the world's GDP annually. Among various protection methods, coating technology remains one of the most effective solutions. Asphalt and tar, both classified as bituminous materials, have long been used as protective coatings for pipelines, bridges, and structural steel. These materials act as physical barriers that isolate the metal from corrosive environments. Steel corrosion in various environments causes many structures to fail too soon. The steel develops rust products, which increase the steel's volume and put stress on the surrounding structure. This results in spalling and cracking, both of which can significantly shorten a member's strength and service life [1]. Corrosion of steel structures is one of the most expensive problems facing engineers in the present world. The structural integrity of many bridges overpasses, parking garages, and other steel-based structures has been impaired by corrosion, and repairs are urgently required to ensure public safety. It is necessary to

develop new and better techniques for the rehabilitation and repair of corroded members as structures near the end of their design life. Accurate detection methods are required to stop corrosion activity in its tracks. Research is constantly being done to assess and apply effective repair techniques due to the growing number of corrosion-related issues in the field of structural design. For many years, steel structures have been strengthened and made more ductile by using polymer-coated inorganic or organic materials. Organic and polymer coatings have been explored and used in recent years to prevent corrosion [2, 3]. The prevention of additional chloride contamination and penetration by the oxygen and water required to continue a corrosion process that has started or caused damage is said to stop corrosion caused by chloride ingress [4,5]. The longevity of a steel structure is influenced by numerous factors. By using appropriate design and maintenance principles and choosing the right materials, corrosion risk can be significantly decreased. Although it is more expensive to use, stainless steel is more resistant to carbonation and chloride penetration. When defining durability, low permeability is essential [6]. Before placing the steel, it is crucial to shield it from chemicals and rain that could corrode it. Even the best steel will corrode in a harsh environment. Steel structures suffer greatly from alternating wet/dry cycles. One of the harshest conditions found in nature, marine exposure speeds up the corrosion process. Deicing salts and other chemicals make it easier for chlorides to penetrate and raise the risk of corrosion [7]. Other elements that accelerate corrosion include high temperatures, contaminated soils, industrial processes, and air pollution. Increasing the resistance of the concrete cover to the penetration of chlorides is the primary measure used in increasing the service life of marine structures [8]. A methodical investigation of the CR of bare and coated X60 pipeline steel in simulated field settings, both with and without a dent or holiday defect, is presented by Xu et al. (2021). To cover a broad range of potential CP conditions that pipeline steel may face in the field, three CP scenarios—no, optimized, and over-protection—were investigated. To simulate various levels of soil corrosivity, two types of salt solutions (sodium chloride or sodium sulfate) with varying temperatures (10 °C, 40 °C, and 65 °C) and pH values (2, 7, and 12) were examined. To show how different factors and their interactions affect the CR of X60 steel, a mathematical model was created. The most crucial element was the state of the coating. It was not demonstrated that the individual effects of other variables, such as temperature, pH, salt composition, and CP, were significant. Rather, the overall CR seemed to be more determined by the interactions between temperature and salt composition, especially the interaction between pH and CP [9]. In addition Al-Gamal et al (2024), PAMAM and ZnO nanoparticles were employed to increase the anti-corrosion property of asphalt binder. Characterization using XRD, <sup>1</sup>H-NMR, and SEM was conducted after the incorporation of varying amounts of PAMAM-ZnO nanocomposites at 1, 2, 4, and 6% by weight into asphalt binder. In this study, with 97.93% corrosion protection efficiency ( $\eta\%$ ) determined using Tafel analysis and a charge transfer resistance (RCT) of 75.91  $\Omega$  cm<sup>2</sup> from EIS results, it was found that an amount of 2% PAMAM-ZnO/asphalt exhibited the best performance. The corrosion inhibition mechanism is driven by sacrificial protection and barrier formation. With its ability to form a homogenous layer on the surface of the carbon steel, the PAMAM-ZnO nanocomposite reduces flaws such as pinholes due to the physical barrier formed that prevents corrosion substances from attacking the metal surface. This sacrificial protective mechanism is attributed to the higher reactivity of the ZnO particles compared with the metal surface, as they preferentially react with corrosive ions such as chlorides. Corrosion products of ZnO are

produced due to such an interaction, resulting in the formation of a protective layer and minimizing the risk of corrosion of the steel surface. Moreover, the application of PAMAM provides a permanent layer of corrosion protection since it helps create a well-distributed adhesion of ZnO in the asphalt matrix. The high corrosion resistance obtained with the 2% PAMAM-ZnO/asphalt composition results from such a synergy of polymer barriers and sacrificial corrosion protection [10]. In order to provide useful information for their industrial applications, this study offers a thorough experimental comparison of the corrosion resistance of tar and asphalt coatings in saline conditions.

## 2. Experimental Procedure

### 2.1 Specimen Preparation

Steel samples measuring 5cm x 2cm x 0.15cm were used in this experiment. Firstly, the samples were cut into the mentioned measurements in order to have consistency during the experiments. Secondly, the samples were polished using emery paper with increasingly fine grits. This would help get rid of the surface impurities, surface roughness, and oxidation, thus giving a smooth surface on which further tests would be performed. Thirdly, the samples were degreased using a solvent that was appropriate for degreasing purposes. This was done so as to get rid of oils and grease from the surfaces since these substances might affect the results of the test.

**Table 1:Chemical composition of the sample**

C	SI	S	P	Mn	Ni	Cu	Cr	Fe
0.17	0.02	0.01	0.01	0.43	0.04	0.05	0.02	Rem.

### 2.2 Preparation and Application of Protective Coatings on Steel Samples

There were two types of protective coatings used in this research: asphalt and tar. They were both properly prepared and then applied evenly on the surface of the steel sample using a paintbrush. The process continued until all the steel samples had an evenly spread protective layer on their surfaces. This was followed by allowing the coatings to dry out completely under room temperature conditions. This was essential for evaluating how effective each of the protective coatings is in preventing corrosion when immersed in the corrosive solutions. In the current study, two kinds of organic/bituminous protective coatings have been utilized, namely, industrial asphalt (penetration grade 60/70) and refined coal tar. For achieving a uniform and appropriate viscosity of these materials, both coatings were independently heated in a temperature-controlled oil bath at  $120\text{ }^{\circ}\text{C} \pm 5\text{ }^{\circ}\text{C}$  while stirring continuously in order to ensure their full liquefaction and homogeneity without causing any thermally-induced decomposition. The liquefied coatings were then applied uniformly on pre-cleaned, degreased and polished steel plates using a dense bristle brush. The application process was carried out following the cross-hatching approach (i.e., horizontal and vertical brush movements). It should be noted that the procedure of coating was carried out at room temperature ( $25\text{ }^{\circ}\text{C} \pm 2\text{ }^{\circ}\text{C}$ ), as well as humidity ( $50\% \pm 5\%$ ). Subsequently, after applying the coating layers, the samples were moved into a dust-free oven, where they were left to dry for 48 hours at room temperature. This treatment time ensures that the coating is dried properly, and no traces of solvent remained within the structure.

In addition, the DFT of the coating was kept within certain bounds . Figure 1 and Figure 2 show the sample before and after coating.

For a comparative evaluation of the physical properties of the coated protective layers, DFT was measured and compared for both the coatings. The average value of the thickness of the stabilized asphalt coating was kept at about  $150 \mu\text{m} \pm \mu\text{m}$ , whereas the average thickness of the tar coating was found to be  $142 \mu\text{m} \pm 12 \mu\text{m}$ . It was observed that the asphalt coating had more visco-elastic and homogenous coverage, effectively covering all the microroughness of the steel surface. On the other hand, the tar coating showed a hard and brittle cross-linking structure after curing. This thickness value is important because it forms a tortuous path for the corrosion reaction species ( $\text{H}_2\text{O}$ ,  $\text{O}_2$ , and  $\text{Cl}^-$  ions).



**Figure 1: steel sample use in study**



**Figure2: sample after coating**

### 2.3 NaCl Solution

Sodium chloride (NaCl) solutions were prepared by dissolving analytical grade NaCl (min 99.5%) in distilled water to reproduce a similar corrosive environment found in the marine atmosphere. In order to prepare solutions using percentage and molarity methods, the exact mass of NaCl to be used was determined. For the preparation of 1% w/v NaCl solution, 10 grams of pure NaCl was dissolved in distilled water to make up the total volume of 1L(1000ml). For preparation of 0.5M and 1.0M solutions, the exact mass of NaCl to be used was determined using the following standard equation in electrolysis:

$$\text{Mass of NaCl (g)} = \text{Molarity (M)} \times \text{Molar Mass of NaCl} \times \text{Volume of solution (L)}$$

The molar mass of NaCl is 58.44 g/mol.

**For 0.5 M NaCl solution (1 Liter):**

$$0.5 \times 58.44 \times 1 = 29.22 \text{ g of NaCl}$$

**For 1.0 M NaCl solution (1 Liter):**

$$1.0 \times 58.44 \times 1 = 58.44 \text{ g of NaCl}$$

Exact quantity of each salt was carefully measured using a high-sensitivity analytical balance and stirred completely using magnetic stirrer.

### 2.4 Corrosion Test and Evaluation of Steel Samples

After the period of immersion in the prepared NaCl solutions, the steel samples were taken out of the solutions. In order to avoid measuring other masses beside corrosion, the samples were first cleaned of any residues, then dried. The initial weight (W1) and the final weight (W2) of the samples were noted after immersion and cleaning process using an analytical balance.

The rate of corrosion for the steel samples was determined by means of the following formula [11]:

$$\text{Corrosion Rate (mm/year)} = (W1 - W2) \times 87.6 / \rho \times A \times T$$

Where:

- W1 = Weight of the steel sample before immersing (g)
- W2 = Weight of the steel sample after immersing and cleaning (g)
- $\rho$  = Density of the steel (g/cm<sup>3</sup>)
- A = Exposed surface area of the steel sample (cm<sup>2</sup>)
- T = Immersion time (hours)

This technique helps to determine the amount of material lost because of corrosion in order to compare the corrosion rates of the two types of materials in different solutions. Using weight losses when analyzing corrosion processes is a common practice in this field because the

amount of corrosion represents the level of material losses in a certain environment. Besides weight losses, the morphological characteristics of samples were considered. It was observed whether there were signs of rust, pitting, etc., on the surfaces. Such observations complement information about corrosion rates. They give more details on how the coatings protect the materials from corrosion, what influence the aggressive environment has on materials, and generally how the corrosion process develops. Overall, these two approaches help to understand the processes occurring in the metal in an aggressive environment better and evaluate the efficiency of using such coatings as asphalt and tar in order to prevent corrosion.

### 2.5 Total Dissolved Solids (TDS) Test

The TDS test was done as part of the experiment in order to determine the amount of dissolved salts in the sodium chloride solutions used in the corrosion experiments. The TDS test determines the amount of organic and inorganic substances present in the solution mainly made up of sodium and chloride ions that play an essential role in the determination of the corrosive nature of the media. The measurement was done using a TDS meter in order to estimate the amount of dissolved solids through the measurement of electrical conductivity of the solution. The higher the TDS level, the greater the amount of dissolved solids in the solution, hence increased susceptibility to the corrosion of steel samples. The test was important to make sure that the levels of salt concentration were consistent at the beginning and throughout the duration of the six days of immersion.

### 2.6 Scanning Electron Microscopy (SEM)

Surface morphology of the steel specimens was analyzed by a Scanning Electron Microscope (SEM) to observe structural modifications after immersion of steel in the NaCl solution. Steel samples, both without coating and coated with asphalt and tar coatings, were prepared by cleaning, drying, and mounting on aluminum stubs using carbon conductive tape. All steel samples were coated with gold prior to SEM analyses in order to improve electrical conductivity. Surface morphologies of the steel samples were obtained at various levels of magnifications (from 500x to 5000x).

## 3. Results and Discussion

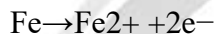
### 3.1 Corrosion Test Results

These steel samples were then joined by threading through the pre-drilled holes and kept inside glass bottles that contained the prepared aqueous solution of NaCl at 1 M and 0.5 M concentration. First of all, all steel samples were weighed before coating them with any material. Four samples were coated with asphalt, and four others were coated with tar. After coating the samples, the samples were again weighed, thus, weighing the difference that came into being after applying coatings on the samples. These samples, with their respective coatings, were immersed in the prepared NaCl solutions. Four samples with asphalt coating and two samples with tar coating were placed in 1 M solution of NaCl. Two asphalt-coated samples and two tar-coated samples were kept in 0.5 M NaCl solution. There were also four control samples which did not have any coating applied on them, out of which two were kept in 1 M and the other two were kept in 0.5 M NaCl solutions. These specimens were kept in the solutions for 72 hours

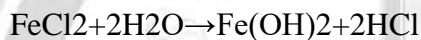
before being removed, cleaned, dried, and weighed to establish their weight reduction due to corrosion. The weighing process was repeated every 72 hours for a total time of 17 days in order to measure the corrosion rate and determine the influence of these coatings. It enabled constant observation of the process of corrosion and its impact on the efficiency of the asphalt and tar coatings[12,13].

### 3.2 Variation of Salt Concentration with Exposure Time

In Figures 3-6, it can be seen that there is a steady decrease in the concentration of salt due to increased corrosion time. This phenomenon can be explained by constant consumption of chloride ions ( $\text{Cl}^-$ ). In the electrolytic reaction of corrosion, iron dissolves according to the following equation:



Ferrous ions combine with chloride ions to form iron chloride ( $\text{FeCl}_2$ ). Further reaction with water causes hydrolysis to produce iron hydroxide ( $\text{Fe}(\text{OH})_2$ ) and hydrochloric acid ( $\text{HCl}$ ):



As these reactions progress, the available chloride ions are gradually consumed, leading to a measurable decline in the overall salt concentration in the surrounding solution. This phenomenon is well-documented in corrosion studies [5,14]. Over extended exposure periods, the rate of salt depletion slows down as corrosion products accumulate on the surface, forming a semi-protective layer that limits the further participation of ions in the reaction.

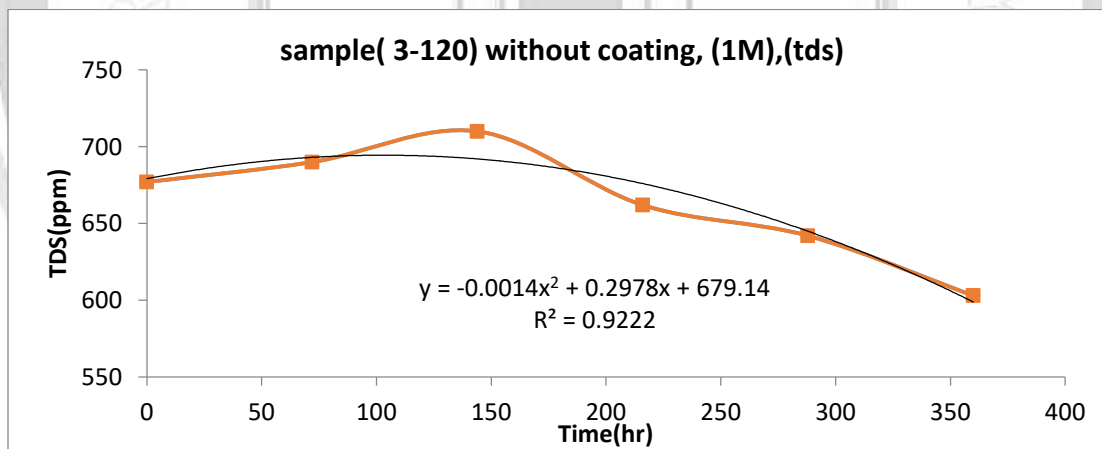


Figure 3: the relationship between the salt concentration and corrosion exposure time .

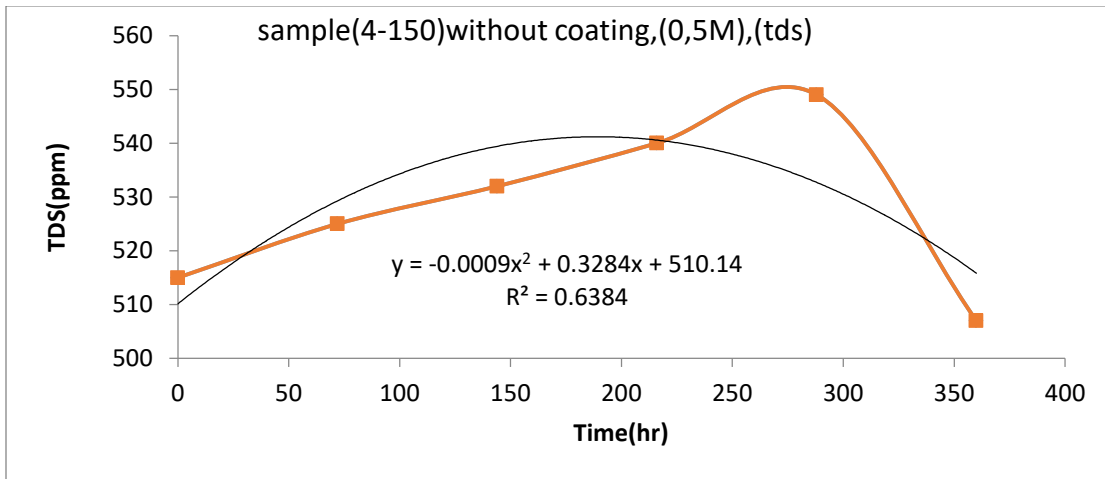


Figure 4: the relationship between the salt concentration and corrosion exposure time .

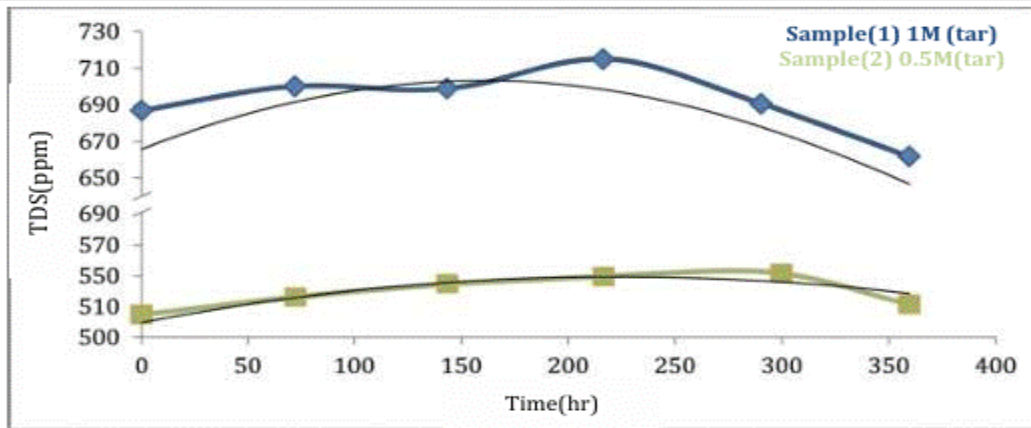


Figure 5: the relationship between the salt concentration and corrosion exposure time .

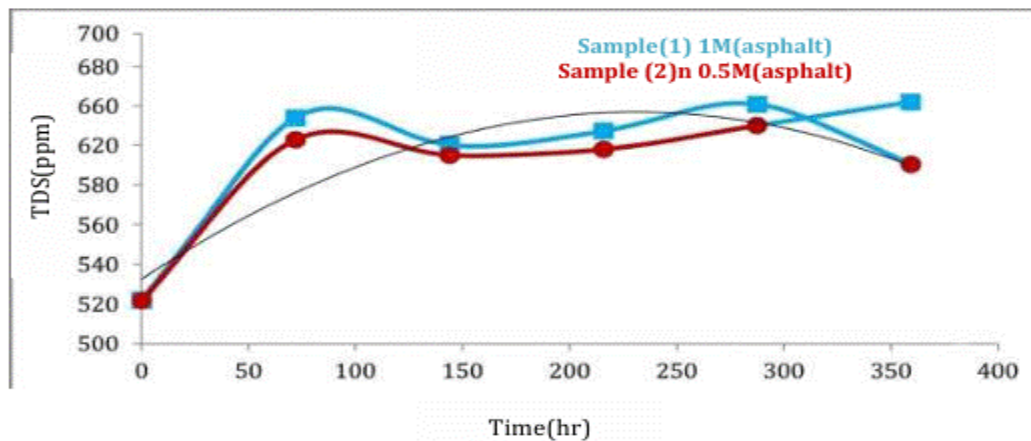


Figure 6: the relationship between the salt concentration and corrosion exposure time .

The exceptional data points in Figures 7 and 8 exceptional data points that do not follow the general trend may result from localized variations in the corrosion behavior. Possible explanations include:

- Localized breakdown of the passive layer, leading to transient increases in corrosion rate (pitting corrosion).
- Surface heterogeneity or microstructural inclusions that create galvanic sites.
- Minor fluctuations in solution composition or temperature during testing [15,16].

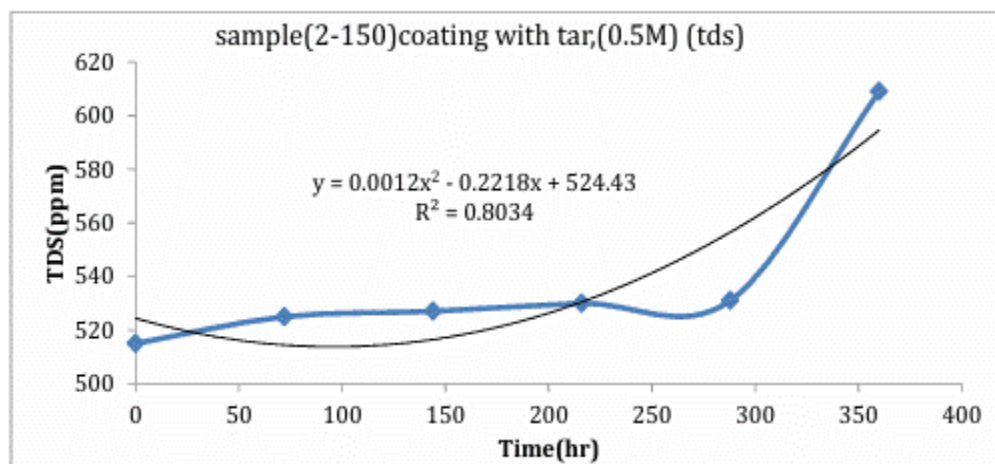


Figure 7: the relationship between the salt concentration and corrosion exposure time .

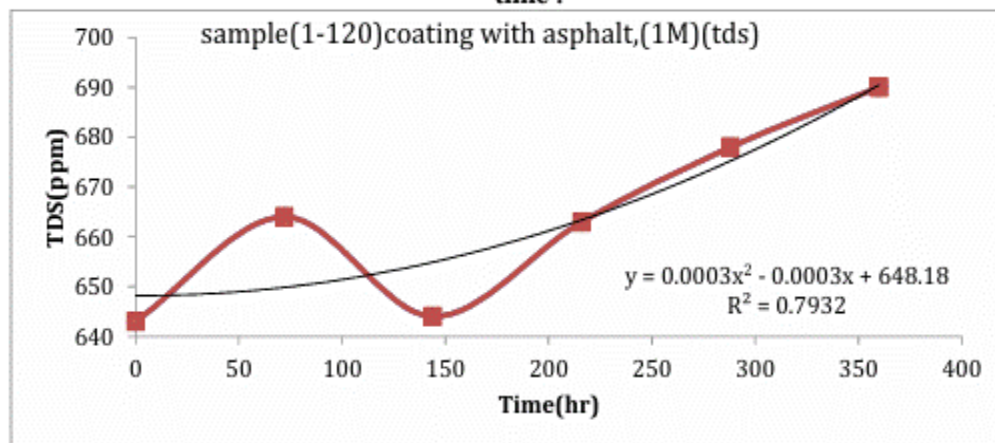


Figure 8: the relationship between the salt concentration and corrosion exposure time .

### 3.3 Corrosion Rate Behavior with Exposure Time

In Figures 9-14 ,a noticeable reduction in the corrosion rate was observed as exposure time increased. This decrease results from the formation of a protective corrosion product film composed mainly of iron hydroxides ( $\text{Fe}(\text{OH})_2$ ,  $\text{Fe}(\text{OH})_3$ ) and iron oxides ( $\text{Fe}_2\text{O}_3$ ,  $\text{Fe}_3\text{O}_4$ ). These

compounds progressively cover the metal surface, acting as a physical and chemical barrier that hinders the transport of oxygen, water, and ions to the underlying metal. This phenomenon, known as passivation, has been widely reported in corrosion engineering literature [6,17]. The initially high corrosion rate is due to the fresh and active metallic surface, but as the passive film develops, the corrosion process transitions into a decelerating regime, leading to a quasi-steady low corrosion rate. The protective film limits the electrochemical reactions at the metal–solution interface, reducing the anodic dissolution of iron and consequently decreasing the overall corrosion rate.

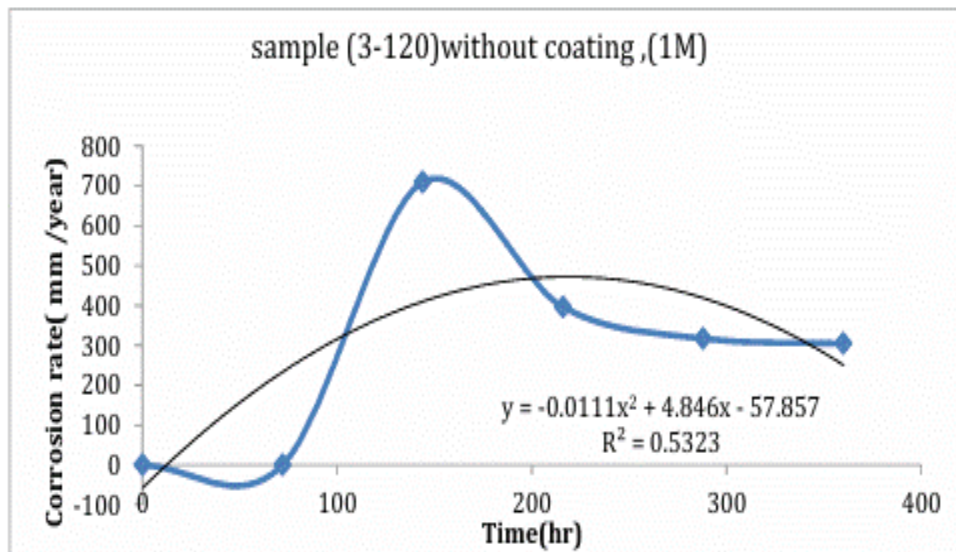


Figure 9: the relationship between the corrosion rate and corrosion exposure time .

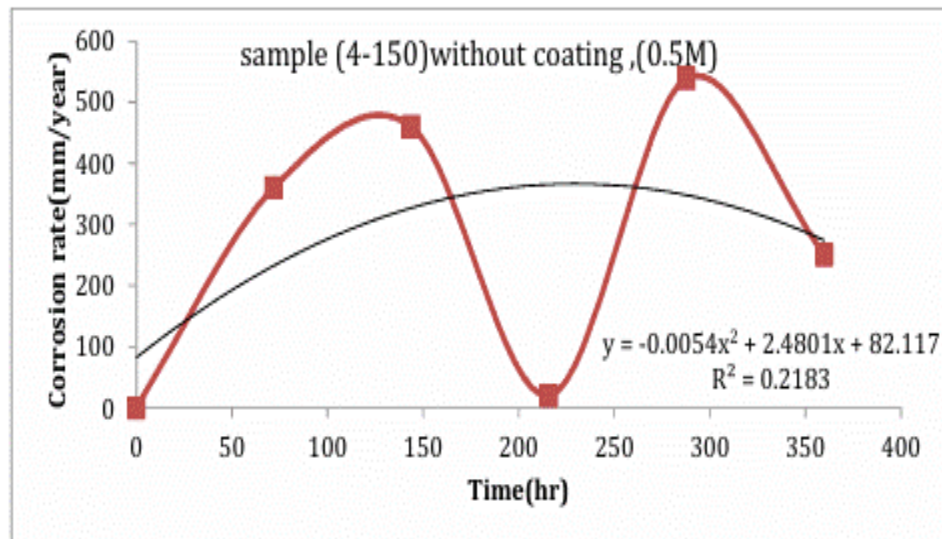


Figure 10: the relationship between the corrosion rate and corrosion exposure time

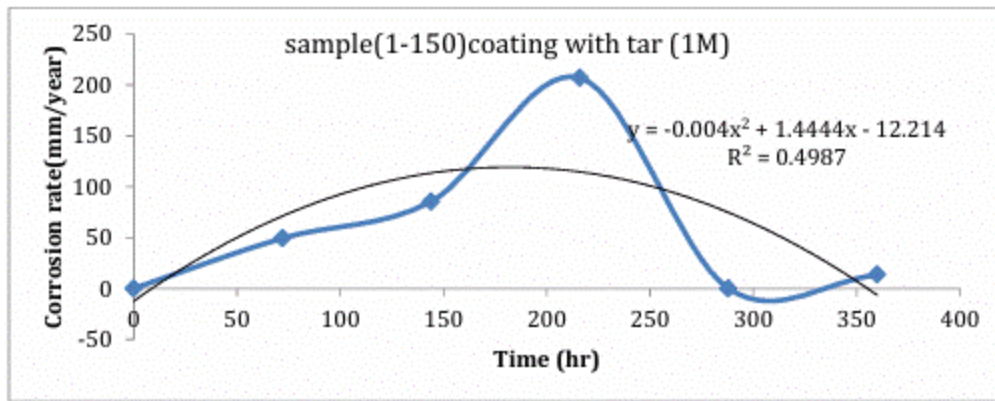


Figure 11: the relationship between the corrosion rate and corrosion exposure time

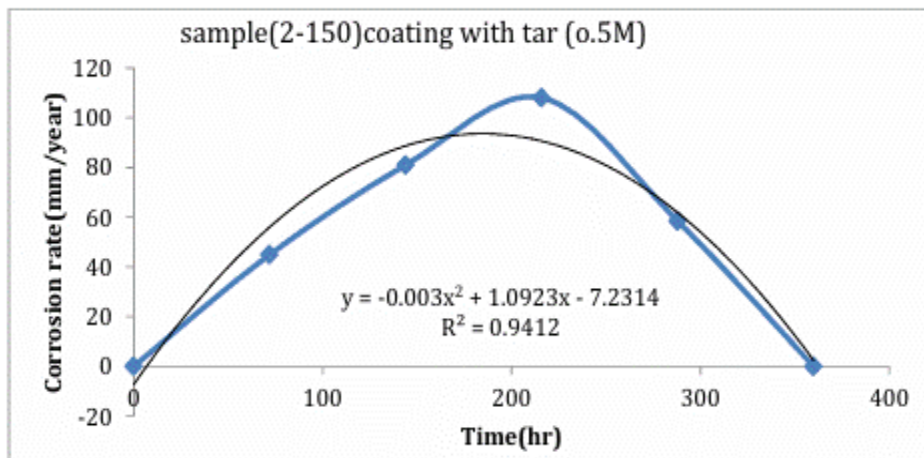


Figure 12: the relationship between the corrosion rate and corrosion exposure time

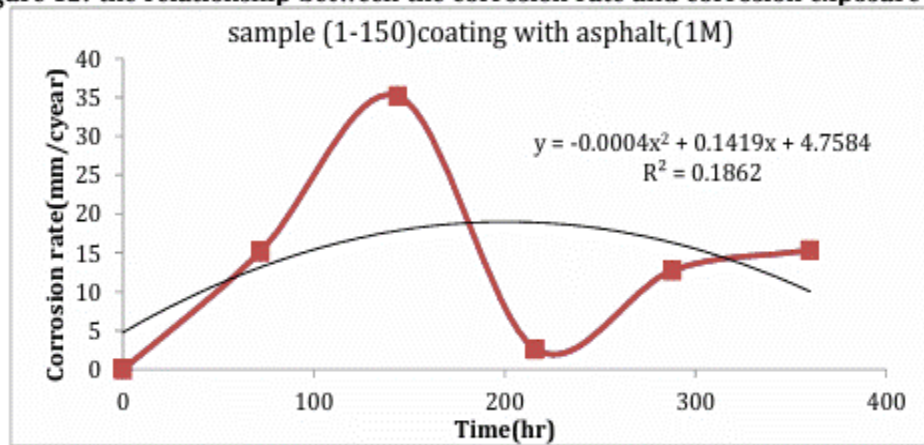


Figure 13: the relationship between the corrosion rate and corrosion exposure time

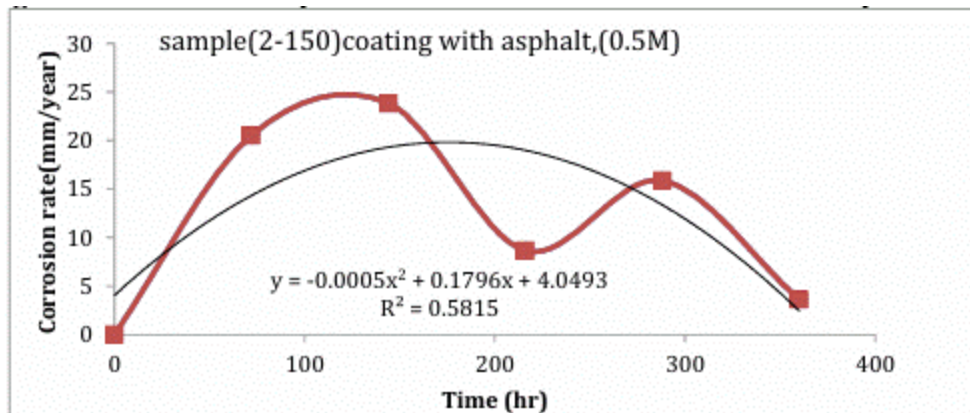


Figure 14: the relationship between the corrosion rate and corrosion exposure time.

Overall, the experimental data suggest that the corrosion process proceeds through three main stages:

1. Initial Active Stage: High corrosion rate and stable salt concentration, dominated by direct metal dissolution in the chloride solution.
2. Stage of transition: Gradual reduction of both salt concentration and rate of corrosion caused by the appearance of corrosion products on the surface of metal.
3. Stage of passivity or steady state: Establishment of the system's quasi-equilibrium state due to the development of the oxide or hydroxide layer that regulates the kinetic processes and causes no variation in parameters.

The presented trend is consistent with the generally recognized principles of carbon steel and iron alloy corrosion in saline environment [5,6,14,17]. Both coating materials have been proven to provide effective protection of steel against corrosion. Nevertheless, corrosion rate in asphalt coated samples has turned out to be lower because of its higher density and adhesiveness compared to tar. Asphalt-coated samples demonstrated the corrosion rate of 0.19 mm/year when being immersed in 0.5 M NaCl and 0.36 mm/year when exposed to 1.0 M NaCl. For tar coatings, the corresponding values have amounted to 0.28 mm/year and 0.52 mm/year, respectively.

Table 2. Corrosion rate comparison for different coatings

Sample Type	NaCl Concentration (M)	Corrosion Rate (mm/year)	Protection Efficiency (%)
Uncoated Steel	0.5	0.86	—
Uncoated Steel	1.0	1.35	—
Tar Coated	0.5	0.28	67.4
Tar Coated	1.0	0.52	61.5
Asphalt Coated	0.5	0.19	77.9
Asphalt Coated	1.0	0.36	73.3

The 'decrease-increase' pattern in the dynamic corrosion characteristics of the coated steel specimens during the entire duration of the test could be scientifically explained through the interaction between two processes, namely the process of passivation, and the degradation of the barrier function. During the first stage of the immersion test, there is a visible decrease in the corrosion rate. This decrease is primarily caused by the formation of a protective layer made of

corrosion products such as iron oxides and iron hydroxides  $\text{Fe}_2\text{O}_3$  and  $\text{Fe}(\text{OH})_3$  on the micro-pathways of the coating that prevent oxygen and moisture from reaching the metal surface. On the other hand, after a certain amount of time, an increase is seen in the corrosion rate. In particular, it is brought about by the accumulation of chloride ions ( $\text{Cl}^-$ ), which penetrate aggressively within the coating due to their small ionic radius. This causes pitting corrosion and, consequently, electro-chemical oxidation of the metal[18].

### 3.4 Microscopic Test Results

The higher effectiveness of asphalt can be explained with regard to the microstructure of this substance – hydrocarbon molecules are contained in it, forming a compact and water-impermeable layer. While tar coatings are quite efficient, they have a higher level of volatility substances that cause the formation of cracks in the coating. Post-immersion visual assessment has shown a considerable amount of rust on the unprotected steel sample, as well as the presence of partial surface corrosion in samples coated with tar. Steel samples covered with asphalt retained their integrity and did not undergo any considerable color changes. Anodic dissolving of iron and cathodic reaction of oxygen reduction can take place at the interface and will be prevented due to the protective properties of the layer. External conditions also play a crucial role; for example, corrosion rates increase with higher concentration of chlorides since passive films break down faster. The performance of the coating mainly depends on moisture resistance and adhesiveness. High viscosity and impermeability allow the use of asphalt coating underwater and underground. The asphalt-coated samples show a more or less continuous coating layer with a smooth-to-near-smooth surface having only a few micropores [19]. There are no significant cracks and detachment of the coating from the steel substrate, signifying good bonding. With increased magnification, several microscopic surface imperfections (micron-sized pores/holes) can be seen, which serve as pathways for the migration of chloride ions should they concentrate there. The tar-coated samples display a somewhat uneven surface compared to asphalt, with thicker and thinner portions, along with blisters or poorly filled in some instances. Tar shows inconsistent performance in terms of corrosion inhibition, with some zones providing adequate protection and other zones showing poor performance (pore/bubbles), allowing  $\text{Cl}^-$  to diffuse across the barrier and corrode the metal. In the case of uncoated (control) samples, there is a homogeneous rust/oxide layer coating the surface, with pits and localized corrosion being observed, especially those areas that were in direct contact with the 1.0M NaCl solution [20]. The production of rust flakes, which can be mechanically removed from the surface easily, is indicative of extreme localized corrosion. The continuous asphalt layer minimizes the openings for the ingress of  $\text{Cl}^-$  into the system and consequently increases the time taken by the  $\text{Cl}^-$  ion to get to the steel, hence the slow corrosion rate by weight. Even though tar serves as an organic shield, the bubbles/crystals accelerate localized corrosion at weak spots[21].

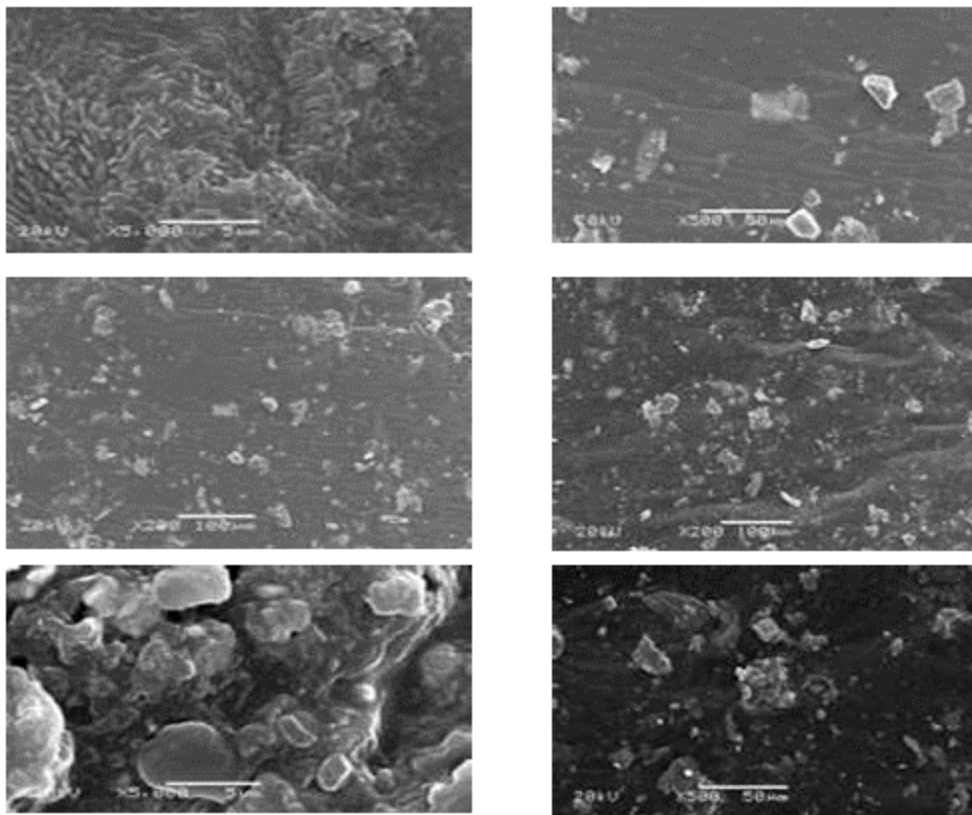


**Figure 15. SEM images of asphalt and tar in a chloride solution at different times and magnifications.**

## 5. Conclusion

Both asphalt and tar coating materials exhibit good corrosion protection performance for steel substrate surfaces subjected to salty media exposure in comparison to unprotected samples, thus serve as a physical protective layer preventing ion penetration. Comparison tests indicate that asphalt coating material, in particular, exhibits superior properties compared to coal tar coating in terms of corrosion protection capacity. Specifically, asphalt coating exhibits lower corrosion rates – 0.19mm/year in 0.5 M NaCl and 0.36 mm/year in 1.0 M NaCl, because of its greater homogeneous viscosity-elasticity property, preventing cracking. The rate of corrosion of the metal substrate surface under coated conditions demonstrates clearly non-linear behavior, namely a decrease- then -increase pattern. In the first stage, this results from the formation of an iron oxide/hydroxide layer, while in the second phase, it results from increased diffusion and breakdown of the passive film. The increase in saline concentration from 0.5 M to 1.0 M NaCl leads to higher corrosion rates.

## References

- [1] M. F. Ibrahim, "Effect of different sodium chloride (NaCl) concentration on corrosion of coated steel," Doctoral dissertation, UMP, 2013.
- [2] B. Hou, X. Li, X. Ma, C. Du, D. Zhang, M. Zheng, et al., "The cost of corrosion in China," *npj Materials Degradation*, vol. 1, no. 1, p. 4, 2017.



- [3] X. Lv, Wang, C., Liu, J., Sand, W., Nabuk Etim, I. I., Zhang, Y., et al., "The microbiologically influenced corrosion and protection of pipelines: A detailed review," *Materials*, vol. 17, no. 20, p. 4996, 2024.
- [4] N. Acharya, R. Sagar, and N. Badi, "Internal Coatings to Prevent Slurry Erosion in Pipelines," in *Slurry Erosion*, Boca Raton, FL, USA: CRC Press, 2026, pp. 166-181.
- [5] G. V. Chilingar, R. Mourhatch, and G. D. Al-Qahtani, *The fundamentals of corrosion and scaling for petroleum & environmental engineers*, Amsterdam, Netherlands: Elsevier, 2013.
- [6] M. A. Ahmed, S. Amin, and A. A. Mohamed, "Current and emerging trends of inorganic, organic and eco-friendly corrosion inhibitors," *RSC Advances*, vol. 14, no. 43, pp. 31877-31920, 2024.
- [7] *Standard Practice for Laboratory Immersion Corrosion Testing of Metals*, ASTM G31-21, 2021.
- [8] S. Rajendran, *Corrosion Science and Engineering*, Boca Raton, FL, USA: CRC Press, 2020.
- [9] M. Xu, H. Liang, Y. Liu, and E. Asselin, "Predicting the External Corrosion Rate of X60 Pipeline Steel: A Mathematical Model," *Metals*, vol. 11, no. 4, p. 583, 2021.
- [10] A. G. Al-Gamal, W. S. Gado, M. A. Abo El-Khair, K. Zakaria, A. A. Ragab, and K. I. Kabel, "ZnO doped PAMAM for asphalt improvement as anti-corrosive coatings," *Scientific Reports*, vol. 14, no. 1, p. 28352, 2024.
- [11] V. R. Rathi, S. D. Nirmal, and S. J. Kokate, "Corrosion study of mild steel, tor steel and CRS steel by weight loss method," *J. Chem. Pharm. Res.*, vol. 2, no. 2, pp. 97–100, 2010.
- [12] Y. Li, H. Qiao, and A. Yang, "Experimental Study on the Protection of an Asphalt Coating to Reinforcement in Magnesium Oxochloride Cement Concrete," *Applied Sciences*, vol. 13, no. 8, p. 4759, 2023.
- [13] M. M. Abdel-Aal, M. S. Abdel-Wahab, E. M. Elsayed, S. I. El-Dek, and M. R. Hussein, "Electrochemical evaluation of EVA/ZnO nanocomposite coatings: achieving superior electrochemical corrosion protection in harsh environments," *RSC Advances*, vol. 15, no. 43, pp. 36414-36427, 2025.
- [14] D. A. Jones, *Principles and Prevention of Corrosion*, Upper Saddle River, NJ, USA: Prentice Hall, 1996.
- [15] L. L. Shreir, *Shreir's Corrosion*, vol. 1. Amsterdam, Netherlands: Elsevier, 2010.
- [16] F. El-Taib Heakal et al., "Corrosion behavior of iron in chloride solutions," *Corrosion Science*, vol. 53, pp. 2728–2737, 2011.
- [17] P. R. Roberge, *Corrosion Engineering: Principles and Practice*, New York, NY, USA: McGraw-Hill, 2008.
- [18] Y. Tang, Z. Fu, P. Zhao, F. Ma, and Y. Hou, "Damage on asphalt surfaces caused by ionic solution erosion and salt crystallization at molecular scale," *Applied Surface Science*, vol. 643, p. 158718, 2024.

- [19] P. Wang et al., *Visual Analysis of the Protective Effect of Asphalt Coating*, Berlin, Germany: Springer, 2022.
- [20] H. Bano et al., "Spatial Evaluation of Preservability of Mild Steel by Coal Tar Epoxy Coatings," *Arabian Journal for Science and Engineering*, 2015.
- [21] P. K. Yadalam, P. Arumugam, S. K. Melanathuru-Balanatha, and C. M. Ardila, "Strontium-Zinc conversion coating on magnesium plates for resorbable tack screws in guided bone regeneration: Characterization and biocompatibility evaluation," *Journal of Clinical and Experimental Dentistry*, vol. 17, no. 8, p. e936, 2025.



## الأداء الوقائي والسلوك البنيوي لطلاءات الأسفلت والقطران على الفولاذ تحت تركيزات مختلفة من الكلوريد

سراء مجيد محمد

قسم الاعمار والمشاريع, الجامعة المستنصرية, بغداد, العراق

saraamajeed96@uomustansiriyah.edu.iq

## الخلاصة

تهدف هذه الورقة البحثية إلى إجراء مقارنة بين تأثيرات تثبيط التآكل لدهانات الأسفلت والقطران المستخدمة على أسطح عينات الفولاذ المعرضة لبيئات كلوريد الصوديوم بتركيزات مختلفة (0.5 مولار و 1.0 مولار). وقد تم ذلك عن طريق طلاء عينات الفولاذ أولاً قبل تعريضها لبيئات كلوريد الصوديوم لمدة 17 يوماً. وأُجريت قياسات لفقدان الوزن للعينات كل 72 ساعة لتقدير معدلات التآكل. كما اعتمدت تقنية قياس الوزن (Gravimetric technique) لتحديد معدل التآكل وفقاً لمعايير ASTM G31-21 وأُجريت اختبارات أخرى مثل اختبار المواد الصلبة الذائبة الكلية (TDS) والمجهر الإلكتروني الماسح (SEM) لدراسة مستويات تركيز الملح والتغيرات في البنية المجهرية للأسطح. ولوحظ وجود انخفاض مستمر في كل من تركيز الأملاح ومعدلات التآكل نتيجة لتشكل طبقة من أكسيد الحديد وهيدروكسيدات على السطح. وقد أظهرت طلاءات الأسفلت مستوى حماية أفضل ضد التآكل مقارنة بطلاءات القطران والعينات غير المعالجة؛ حيث بلغت قيم معدلات التآكل 0.19 ملم/سنة في محلول NaCl بتركيز 0.5 مولار و 0.36 ملم/سنة في محلول 1.0 مولار، بينما بلغت في حالة طلاءات القطران 0.28 ملم/سنة و 0.52 ملم/سنة على التوالي. وكشفت صور المجهر الإلكتروني الماسح (SEM) أن طلاء الأسفلت كان كثيفاً ومتجانساً وشديداً الالتصاق بالسطح مع وجود عيوب قليلة، بينما تميز طلاء القطران بوجود شقوق مجهرية ومسامية. الكلمات الدالة: التآكل؛ طلاء الأسفلت؛ طلاء القطران؛ حماية الفولاذ؛ محلول كلوريد الصوديوم (NaCl)؛ معدل التآكل؛ المواد القارية (البيثومينية)